# Linearity and additivity in cluster-induced sputtering: A molecular-dynamics study of van der Waals bonded systems

Christian Anders and Herbert M. Urbassek*
*Fachbereich Physik, Universität Kaiserslautern, Erwin-Schrödinger-Strasse, D-67663 Kaiserslautern, Germany*

Robert E. Johnson
*Department of Nuclear Engineering and Engineering Physics, University of Virginia, Charlottesville, Virginia 22901*
(Received 9 February 2004; published 13 October 2004)

Using molecular-dynamics simulation, we study sputtering of a condensed-gas solid induced by the impact of atomic clusters with sizes $1 \leqslant n \leqslant 10^4$. Above a nonlinear onset regime, we find a linear increase of the sputter yield $Y$ with the total energy $E$ of the bombarding cluster. The fitting coefficients in the linear regime depend only on the cluster size $n$ such that for fixed bombardment energy, sputtering decreases with increasing cluster size $n$. We find that to a good approximation the sputter yield in this regime obeys an additivity rule in cluster size $n$ such that doubling the cluster size at the same cluster velocity amounts to doubling the sputter yield. The sputter-limiting energy $\epsilon_s$ is introduced which separates erosion ($\epsilon > \epsilon_s$) from growth ($\epsilon < \epsilon_s$) under cluster impact.

DOI: 10.1103/PhysRevB.70.155404 PACS number(s): 79.20.Rf, 79.20.Ap, 61.80.Lj

## I. INTRODUCTION

The irradiation of solids by energetic clusters has been investigated in the last decade both experimentally and theoretically.[1–3] Because of potential applications in the fields of cluster deposition of materials, thin-film growth, implantation, or surface cleaning, mostly metallic and covalently bonded targets have been studied,[3–7] while investigations of weakly bonded target materials are rare. However, cluster irradiation of the latter class of target systems also finds important applications. Here we mention in particular applications in the outer solar system where many objects, such as the moons of the giant planets and comets, consist of ices or are covered with ices. The interaction of dust particles or—in the case of planetary ring systems—of small ice particles with such surfaces affects an important issue to understand the evolution (erosion or growth) of these bodies.[8,9] Another application lies in the field of matrix-isolation spectroscopy,[10] where reactive chemical species are embedded in a frozen-gas matrix. Irradiation with atoms or clusters may be used to set these radicals free and to study their properties in the gas phase.

The physics of cluster-solid interaction offers interesting questions of fundamental character. A prominent example is the question of the linear or non-linear character of the interaction process. This question is often asked within the context of collision-cascade theory: Can the collision cascade induced by the cluster impact in the target be understood as the superposition of the collision cascades induced by the individual cluster atoms? This aspect has been studied to some degree; in general it has been found that the cluster-surface interaction process is non-linear.[11,12] Here we consider the concept of linearity in a more general and simpler sense: namely, as the linearity of the sputter yield with respect to the total cluster energy. We shall also inquire into the additivity in cluster-induced sputtering: To what extent can the sputter yield induced by a cluster of size $n$ be determined as the sum of the sputter yields induced by equi-velocity clusters of size $n_1$ and $n_2$ with $n = n_1 + n_2$?

In the present article, we report on simulations of a model system. The potential is chosen to reproduce the interaction of Ar clusters with a frozen Ar target. However, since the low-energy interaction is well described by a Lennard-Jones potential, our results may prove fruitful to understand the interaction of a wider class of weakly bonded solids. A particularly intriguing aspect of the Lennard-Jones potential is its simple scaling properties; in our case, the sputter yield will depend only on the cluster impact energy scaled to the cohesive energy of the solid, and the number of atoms in the cluster. Due to this simple scaling property, these model calculations are valuable also beyond the particular case studied, i.e., $\mathrm{Ar} \rightarrow \mathrm{Ar}$ impacts. This scaling has been examined, for instance, for sputtering following the excitation of a cylindrical track in a solid.[13]

## II. METHOD

We bombard a large target containing $N$ atoms with a cluster containing $n$ atoms, $n \ll N$. $N$ varies between 19 000 and 1 280 000 atoms. The target size was adapted to the size and energy of the bombarding cluster. The target was created in an amorphous structure by slowly quenching from the melt.[14–16] An amorphous target structure was chosen in order to remove any effects of target crystallinity. The projectile clusters also have an amorphous structure; they were created by cutting out a roughly spherical cluster containing exactly $n$ atoms from the amorphous bulk structure. Both target and cluster were relaxed before the simulation was begun.

Target and cluster atoms are considered to be of the same material. They interact via the Lennard-Jones potential

$$\Phi(r) = 4\epsilon_0 \left[ \left( \frac{r}{\sigma} \right)^{12} - \left( \frac{r}{\sigma} \right)^{6} \right]. \quad (1)$$

The energy scale $\epsilon_0 = 10.32$ meV and the length scale $\sigma = 3.405$ Å are appropriate for Ar.[17,18] The potential is cutoff at $r_c = 2.5\sigma$ where the potential is smoothly reduced to zero

 

via a Tersoff function.[19] Toward higher interaction energies, the Lennard-Jones potential is smoothly joined to the KrC interaction potential,[20] which sufficiently well describes Ar-Ar interaction at small separations. A spline interpolates the potentials between around 0.03 and 1.5 eV.[15] The mass of all atoms has been assumed to be that of Ar, $m=40$ amu. Note that all low-energy processes are described by the Lennard-Jones potential and hence its three parameters $\epsilon_0$, $\sigma$, and $m$.

Instead of the bond energy $\epsilon_0$, we shall use the cohesive energy $U$ to parametrize our results,

$$U = \frac{1}{2N} \sum_{\substack{i,j \\ i \neq j}} \Phi(r_{ij}), \tag{2}$$

where $r_{ij}$ are the interatomic distances in the solid. We shall use $U=7.9\epsilon_0$, as it is appropriate for our truncated Lennard-Jones potential in a fcc structure.[21] We note, however, that the amorphous structure is more loosely bound with a cohesive energy of $U \approx (6.9\text{-}7.0)\epsilon_0$. Due to the scaling properties of the Lennard-Jones potential, our results pertaining to low-energy processes can be easily scaled to other materials; the scaling does, however, not apply to high energy processes where the KrC potential dominates, i.e., the stopping of the cluster.

Our molecular-dynamics scheme employs the Verlet algorithm in velocity form for time integration.[22] The time step is automatically adapted; it ranges from 0.3 fs in the initial phase of the bombardment to 1 fs in the later thermalized phases. Our results are based on averages over several irradiation events, which differ by the exact location of the cluster impact point and its orientation; this allows us to estimate the statistical accuracy of the simulations. Thus, for $n=1$, we average over 25 impacts and for $n=4$ over 15 impacts, while for larger clusters, $4<n\leqslant 13$, our results are based on 5 events. For even larger clusters, our results are based on single events. Our simulations run for 20 ps; an inspection of the time evolution of the sputter yield suggests this time to be sufficiently long. Only for the largest cluster size $n=10^4$, the simulation proceeds until $t=40$ ps. In the latter half of this simulation time, between 20 and 40 ps, these sputter yields still continue increasing. As a consequence, our data for this cluster size are lower limits, and will only be used for qualitative argumentation.

## III. RESULTS

### A. Sputter yield

We define the sputter yield $Y$ as the number of atoms emitted from the cluster-irradiated surface, irrespective of whether the atoms originate from the target or the cluster material. Since we simulate self-irradiation, this criterion corresponds to the experimental procedure. In detail, our sputter detector counts all those atoms which have left the interaction spheres of the atoms remaining in the target.

For a pure Lennard-Jones potential, $\epsilon$, $\sigma$, and $m$ are the only material parameters of the system. Since the sputter yield $Y$ is a dimensionless quantity and hence can only depend on dimensionless quantities, the sputter yield of a projectile cluster of size $n$ and energy $E$ can only depend on $\epsilon$ and $n$, where $\epsilon$ is the scaled bombarding energy,

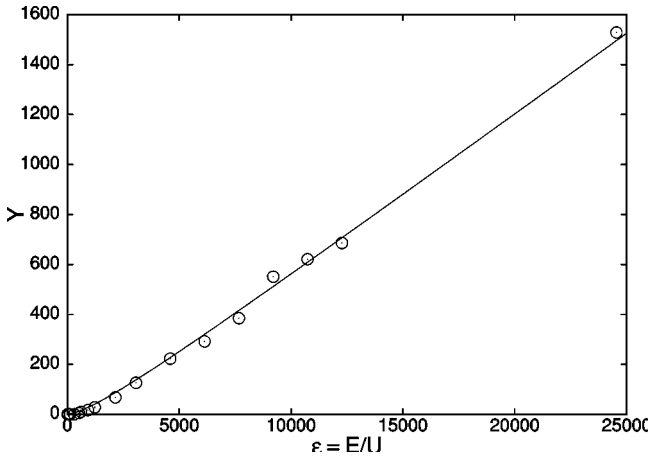


FIG. 1. Sputter yield $Y$ vs scaled bombarding energy $\epsilon$ for $Ar_{100}$ cluster bombardment.

$$\epsilon = \frac{E}{U}. \tag{3}$$

In our simulation, all low-energy processes are described by the Lennard-Jones potential. Insofar as the high-energy stopping of the cluster—here governed by the Kr-C potential—is only important for the energy deposition and not so much for atom emission, our results should be valid for all self-sputtering experiments on weakly bonded materials.

Figure 1 presents the simulated sputter yields for the special case of $Ar_{100}$-bombardment as a function of the scaled bombarding energy $\epsilon$. Toward high energies, $Y$ increases linearly with the bombarding energy, while for small energies, an *onset regime* is apparent. We attempt a fit of this dependence with the expression

$$Y = \alpha \frac{\epsilon^{1+b}}{(\epsilon_c + \epsilon)^b}, \tag{4}$$

which reduces to

$$Y = \alpha \epsilon_c \epsilon^{1+b}, \ \epsilon \ll \epsilon_c, \tag{5}$$

for small $\epsilon \ll \epsilon_c$, and to a linear dependence

$$Y = \alpha(\epsilon - b\epsilon_c), \ \epsilon \gg \epsilon_c, \tag{6}$$

for large $\epsilon \gg \epsilon_c$. We note that linear energy dependencies above a threshold energy, similar to Eq. (6), have been observed earlier in the context of crater formation, plastic surface deformation, and target atom displacements induced by cluster impact on metal and Si surfaces.[23–25]

The exponent $b$ describes the nonlinear onset regime, $\epsilon_c$ is the critical threshold energy separating the onset and the linear regimes, and $\alpha$ has the meaning of a sputter efficiency. Our best fit for $n=100$ gives the parameters $\alpha = 0.065 \pm 0.001$, $\epsilon_c = 3160 \pm 480$, $b = 0.54 \pm 0.03$; this fit curve is included in the figure.

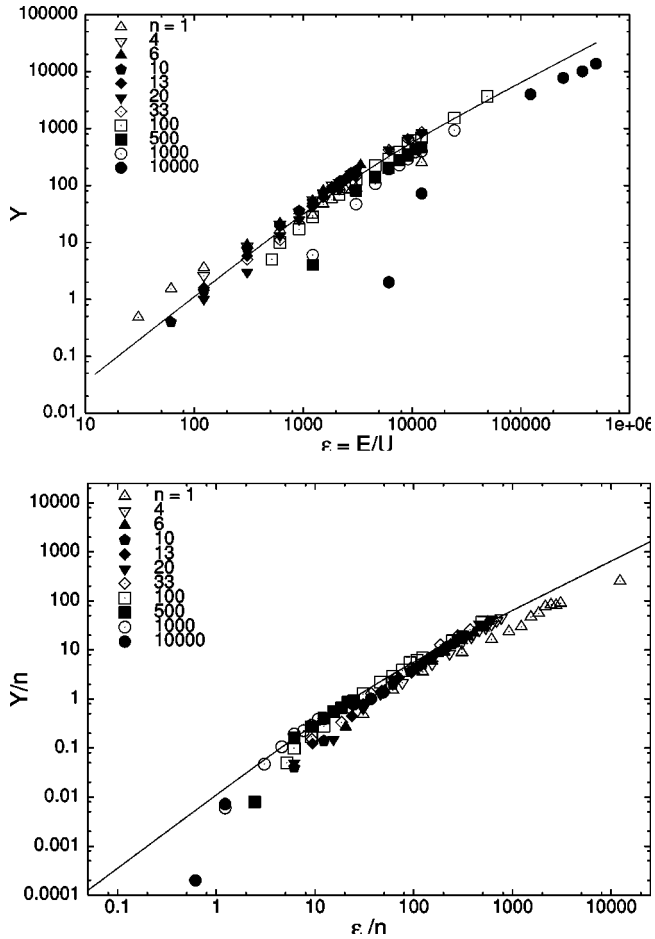


FIG. 2. (a) Synoptical display of sputter yield $Y$ vs scaled bombarding energy $\epsilon$ for projectile clusters of various size $n$, see legend. A fit function according to Eq. (4), with parameters as appropriate for $n=100$, is included. (b) Same data plotted as $Y/n$ vs $\epsilon/n$.

Figure 2(a) gives a synoptical view of all sputter yields calculated. Data are included for $1 \leqslant n \leqslant 10^4$. While the data generally align around the fit curve (as taken from Fig. 1), still a significant spread in the data can be seen—in particular for the largest projectile cluster size, $n=10\,000$. This spread can be diminished by displaying the yield per projectile atom, $Y/n$, versus the projectile energy per atom, $\epsilon' = \epsilon/n$. Note that the dependence, Eq. (4), can then be written as

$$\frac{Y}{n} = \alpha \frac{\epsilon'^{1+b}}{(\epsilon_c' + \epsilon')^b}. \tag{7}$$

Here $\epsilon_c' = \epsilon_c/n$ has been introduced. Figure 2(b) displays our simulation data $Y/n$ versus $\epsilon/n$. Except for the case of monomer bombardment ($n=1$) and for very small $\epsilon/n \lesssim 2$, the data appear to converge and are well fit by a single curve which is adequately described by our best fit for $n=100$. Note also that the data appear to converge increasingly better with increasing $\epsilon/n$.

A sputter yield given by the form $Y=nf(\epsilon')$, cf. Eq. (7), in which $f(\epsilon')$ contains no explicit $n$-dependence describes an *additive* behavior. That is, only the energy per atom, in other words the projectile velocity, describes the contribution of the projectile atom to the total sputter yield. Doubling the projectile size for the same velocity will hence double the sputter yield. This additivity has not been described in earlier investigations of cluster-induced sputtering.

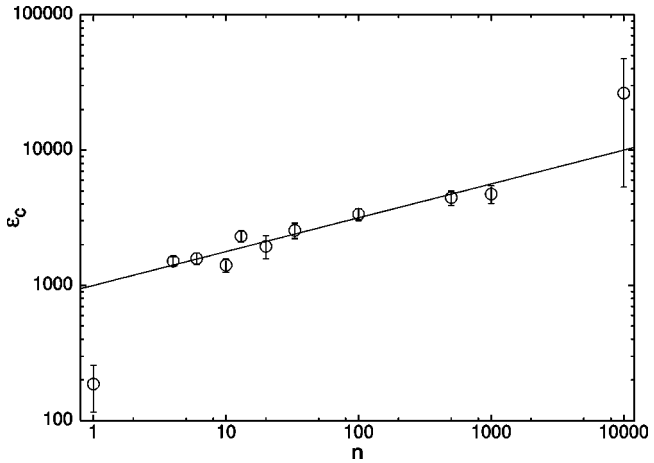


FIG. 3. The critical energy $\epsilon_c$ separating the onset and the linear regimes vs projectile cluster size $n$. A law $\epsilon_c \propto n^{0.25}$, Eq. (8), has been included to guide the eye.

### B. Discussion of parameters

Fitting each of the data sets for a given $n$ using Eq. (4), Fig. 3 displays our simulation data for the critical energy $\epsilon_c$ separating the onset and the linear regimes. A steady increase of $\epsilon_c$ with $n$ is seen, which roughly follows an $n^{0.25}$ dependence,

$$\epsilon_c(n) = 1000 n^{0.25}. \tag{8}$$

The sputter efficiency $\alpha$ indicates how efficient the available impact energy $\epsilon$ can be used to produce ejecta. The projectile size dependence of $\alpha$ is displayed in Fig. 4. $\alpha$ has a maximum in the range of $20 < n \lesssim 30$. For larger cluster sizes, $\alpha$ drops monotonically and reaches a value of around 0.03 for $n=10^4$. $\alpha$ also decreases toward small cluster sizes and reaches a similar value, $\alpha=0.035$, for $n=1$. We estimate

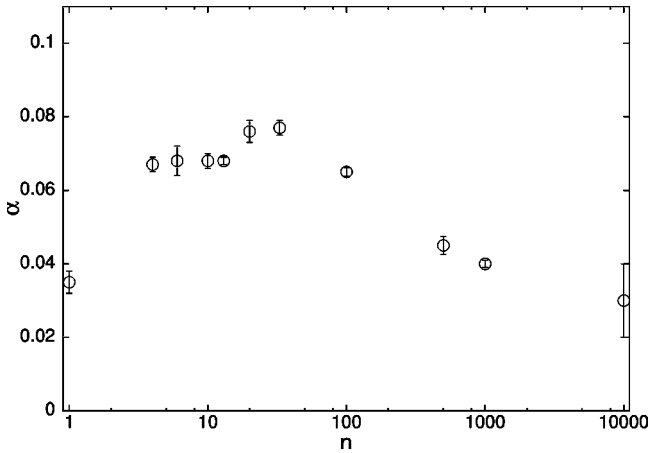


FIG. 4. Sputter efficiency $\alpha$ vs projectile cluster size $n$.

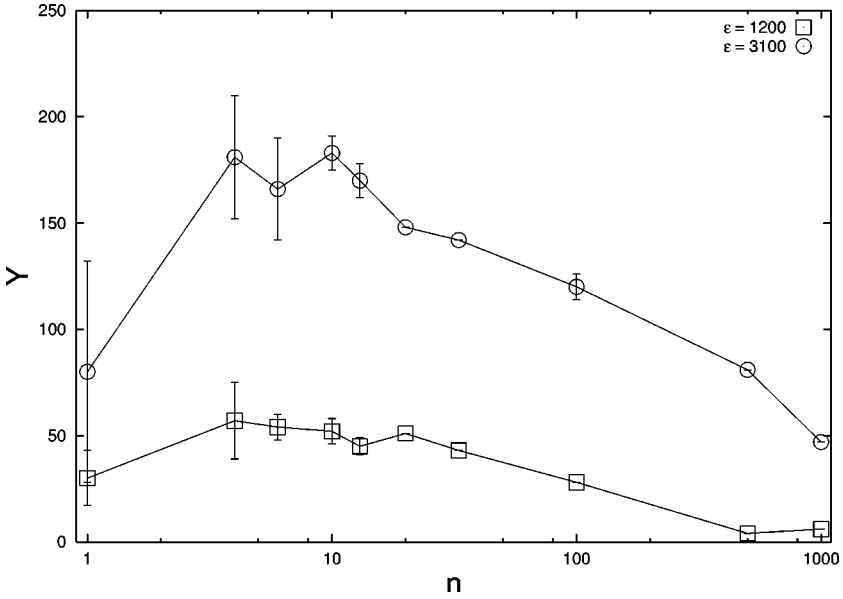


FIG. 5. Sputter yield $Y$ at fixed total bombarding energy $\epsilon$ vs projectile cluster size $n$. Lines are to guide the eye.

the accuracy of our sputter yields to around 10% (except for $n=10^4$) with a similar accuracy for the value of $\alpha$.

Note that the maximum of the efficiency $\alpha$ at values of $n\cong 20-30$ does not lead to maximum sputter yields for this cluster size at a given $\epsilon$, since the term $\alpha\epsilon$ is counteracted by the effect of the sputter threshold. Figure 5 demonstrates this by displaying the sputter yield at fixed total energy $\epsilon$ as a function of the cluster size. A broad maximum for cluster sizes between $4\leqslant n\leqslant 10$ can be seen both for $\epsilon=1200$ and 3100. For small projectiles, in particular monomers, $n=1$, the sputter yield decreases since monomers tend to deposit their energy deep inside the solid, causing little sputtering. For large projectiles, the sputter yield again decreases, since the available energy is distributed on more and more projectile atoms.

In view of the discussion of Eq. (7), the main dependence of $Y/n=f(\epsilon/n)$ on $n$ is contained in $\alpha$. Therefore, the shape of the yield curve in Fig. 5 reflects quite closely that of the sputter efficiency in Fig. 4.

Finally, Fig. 6 displays the fit values for the exponent $b$ obtained from our simulation data. Its value lies in the range $0.35\leqslant b\leqslant 0.55$. However, a value $b=0.5$ appears to be a good representation of the data and will be adopted for further discussion.

### C. Connection to collision-cascade sputtering: Linearity and additivity

Collision-cascade sputtering is described by

$$Y(E)\propto\frac{S_n(E)}{U}, \tag{9}$$

where $S_n$ is the nuclear elastic (knock-on) stopping cross section. For a Kr-C potential, at the energies investigated

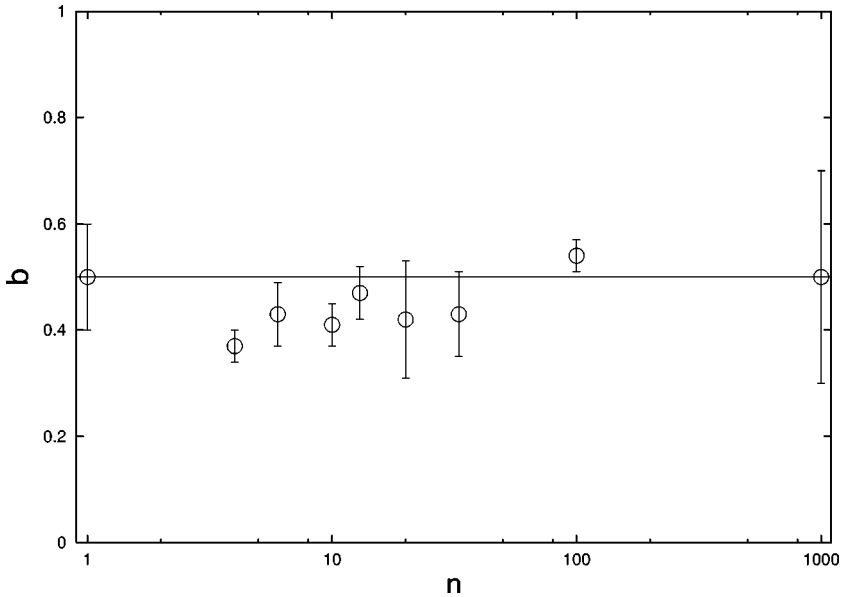


FIG. 6. Power exponent $b$ of nonlinear onset regime.

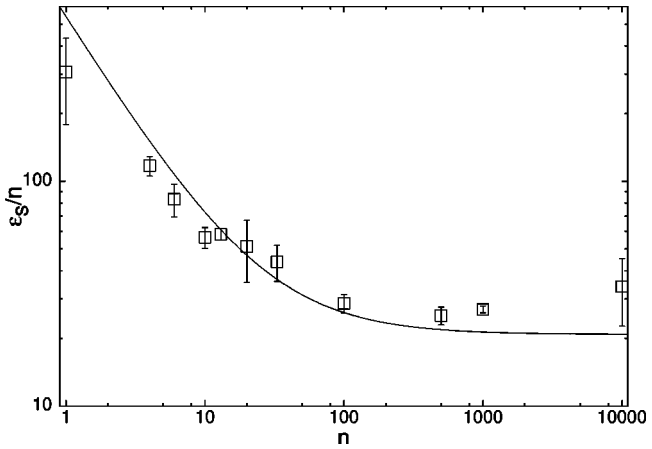


FIG. 7. Erosion limit $\epsilon_s/n$ vs projectile cluster size $n$. The limit is defined as the energy $\epsilon_s$ necessary to sputter $n$ atoms. Line: model, Eq. (11).

here, the stopping cross section scales[26,27] as $S_n \propto E^{2/3}$. Thus collision cascade sputtering predicts a somewhat slower than linear increase of the sputter yield with bombarding energy. This is in contrast to our simulation data at low energies, and gives evidence of the well known fact[14,28] that sputtering of condensed-gas targets in the knock-on regime does not result from the standard collision-cascade mechanism involving binary collisions between a moving atom and a stopped atom.

The linearity of $Y$ with the stopping cross section $S_n$ is a distinctive feature of collision-cascade sputtering and has also been termed linear sputtering. Any deviation from Eq. (9) has been termed non-linear sputtering.[29,30] Our results for cluster impact on a condensed-gas target cannot be described as linear sputtering, in the sense of Eq. (9). However, they obey an additivity rule in the cluster size $n$ as described in the discussion of Eq. (7) above. Also, for fixed $n$, they are linear in the total impact energy $E$. In summary, our cluster impact studies describe a region which—despite being quite distinct from the well-established collision-cascade sputtering—is described by the simple features of linearity in energy and additivity in cluster size.

### D. Sputter-limiting energy

For several applications, it is of interest to find the energy $\epsilon_s$, which separates growth and erosion of the target induced by cluster bombardment. We define this limit by

$$Y(\epsilon_s) = n, \tag{10}$$

and call $\epsilon_s$ the sputter-limiting energy. We note that an analogous sputter- or erosion-limiting energy has been considered recently in the context of Au-cluster-induced sputtering of a Au target.[31]

Thus, for $\epsilon < \epsilon_s$, cluster bombardment will induce growth (i.e., more incident atoms will stick than atoms are ejected) while for $\epsilon > \epsilon_s$, it will induce erosion. Figure 7 displays the values of $\epsilon_s$ as extracted from our simulations. $\epsilon_s/n$ is seen to be monotonically descreasing with cluster size $n$. This decrease appears to saturate above $n \geqslant 100$ at $\epsilon_s/n \cong 25-30$.

Using Eq. (10) in the linear description of sputter yields at large $\epsilon$, Eq. (6), we find

$$\frac{1}{n}\epsilon_s = \frac{1}{\alpha} + \frac{b\epsilon_c}{n}. \tag{11}$$

This relationship is also displayed in Fig. 7. We see that the constant value at large $n$ of $\epsilon_s/n = 1/\alpha \cong 25-30$ for $n \gtrsim 100$ is consistent with the linear increase of the sputter yield with total cluster energy. The increase of $\epsilon_s/n$ toward small $n$ is seen to be due to the decrease in sputter efficiency with decreasing $n$ at small $n$.

## IV. CONCLUSIONS

Using Ar as an example of a van der Waals bonded material, we studied the sputtering produced by incident cluster projectiles over a wide range of bombarding energies. We created amorphous solids and clusters bonded by the Lennard-Jones potentials with KrC cores. The incident energy $E$ was scaled by the cohesive energy $U$, $\epsilon = E/U$, and values of $\epsilon$ ranging from 100 up to $5 \times 10^5$ and cluster sizes $n$ between 1 and $10^4$ were considered. For the Lennard-Jones potential, the sputter yield depends only on the scaled energy $\epsilon$ and the cluster size $n$. Therefore, we investigate this scaling behavior with the help of molecular-dynamics simulation. We find:

1. Above a threshold $\epsilon_c \cong 1000 n^{0.25}$, the sputter yield $Y$ increases linearly with the scaled energy of the impacting cluster, $\epsilon$: $Y \cong \alpha(\epsilon - b\epsilon_c)$.

2. Below the threshold, the yield depends nonlinearly on $\epsilon$, $Y \propto \epsilon^{1.5}$.

3. An analytical expression, unifying the linear and the onset sputter regimes has been found which describes the simulation data over a broad range of energies.

4. The details of the functional forms $\alpha(n)$ and $\epsilon_c(n)$ can be deduced from our simulations. While $\epsilon_c$ slowly increases like $\epsilon_c \propto n^{0.25}$, $\alpha$ exhibits a maximum at $n \cong 10$, slowly decreasing toward small and large cluster sizes.

5. We introduce a sputter-limiting energy $\epsilon_s$. It indicates the boundary between erosion ($\epsilon > \epsilon_s$) and growth ($\epsilon < \epsilon_s$) of the solid under cluster bombardment. We find $\epsilon_s/n \cong 25-30$ for $n \geqslant 100$, while $\epsilon_s$ increases toward smaller cluster sizes so that even relatively energetic small clusters can lead to growth.

For the van der Waals solids studied, the collision-cascade model fails even for individual energetic heavy ions like the incident Ar-atom studied here. That is, the concept of low-energy binary collisions in the solids fails. Therefore, it is also not surprising that the collision cascade model fails for impacting clusters. Such a failure has often been termed nonlinear sputtering.

However, it has been shown here that the yield due to cluster impact is essentially linear in the incident energy above an energy threshold that depends slowly on cluster size. Furthermore, the sputter yield is additive in the cluster

size for a given impact velocity. Therefore, for cluster ion impact of solids we prefer not to use the traditional terminology distinguishing linear versus nonlinear sputtering. Rather we change the paradigm and refer to linear sputtering as a sputter yield that increases nearly linearly with the available cluster impact energy. This regime is in contrast to the low-energy threshold or onset regime which is nonlinear in the deposited energy.

*Electronic address: urbassek@rhrk.uni-kl.de; URL: http://www.physik.uni-kl.de/urbassek/

[1] H. Haberland, Z. Insepov, and M. Moseler, Z. Phys. D: At., Mol. Clusters **26**, 229 (1993).
[2] M. Ghaly and R. S. Averback, Mater. Res. Soc. Symp. Proc. **279**, 17 (1993).
[3] Z. Insepov and I. Yamada, Nucl. Instrum. Methods Phys. Res. B **99**, 248 (1995).
[4] I. Yamada, J. Matsuo, Z. Insepov, D. Takeuchi, M. Akizuki, and N. Toyoda, J. Vac. Sci. Technol. A **14**, 781 (1996).
[5] Z. Insepov and I. Yamada, Nucl. Instrum. Methods Phys. Res. B **121**, 44 (1997).
[6] Z. Insepov, I. Yamada, and M. Sosnowski, Mater. Chem. Phys. **54**, 234 (1998).
[7] I. Yamada, J. Matsuo, Z. Insepov, T. Aoki, T. Seki, and N. Toyoda, Nucl. Instrum. Methods Phys. Res. B **164–165**, 944 (2000).
[8] R. E. Johnson, *Energetic Charged-Particle Interactions with Atmospheres and Surfaces* (Springer, Berlin, 1990).
[9] S. Jurac, M. A. McGrath, R. E. Johnson, J. D. Richardson, V. M. Vasyliunas, and A. Eviatar, Geophys. Res. Lett. **29**, 2172 (2002).
[10] D. E. David and J. Michl, Prog. Solid State Chem. **19**, 283 (1989).
[11] V. I. Shulga, M. Vicanek, and P. Sigmund, Phys. Rev. A **39**, 3360 (1989).
[12] R. Heinrich and A. Wucher, Nucl. Instrum. Methods Phys. Res. B **207**, 136 (2003).
[13] E. M. Bringa, M. Jakas, and R. E. Johnson, Nucl. Instrum. Methods Phys. Res. B **164–165**, 762 (2000).
[14] H. M. Urbassek and K. T. Waldeer, Phys. Rev. Lett. **67**, 105 (1991).
[15] K. T. Waldeer and H. M. Urbassek, Nucl. Instrum. Methods Phys. Res. B **73**, 14 (1993).
[16] H. M. Urbassek, H. Kafemann, and R. E. Johnson, Phys. Rev. B **49**, 786 (1994).
[17] A. Michels, H. Wijker, and H. K. Wijker, Physica (Amsterdam) **15**, 627 (1949).
[18] J.-P. Hansen and L. Verlet, Phys. Rev. **184**, 151 (1969).
[19] J. Tersoff, Phys. Rev. B **38**, 9902 (1988).
[20] W. D. Wilson, L. G. Haggmark, and J. P. Biersack, Phys. Rev. B **15**, 2458 (1977).
[21] N. W. Ashcroft and N. D. Mermin, *Solid State Physics* (Saunders, Philadelphia, 1976).
[22] D. Heermann, *Computer simulation methods in theoretical physics* (Springer, Berlin, 1990), 2nd ed.
[23] R. Aderjan and H. M. Urbassek, Nucl. Instrum. Methods Phys. Res. B **164–165**, 697 (2000).
[24] Y. Yamaguchi and J. Gspann, Phys. Rev. B **66**, 155408 (2002).
[25] T. Aoki, J. Matsuo, and G. Takaoka, Nucl. Instrum. Methods Phys. Res. B **202**, 278 (2003).
[26] M. Vicanek and H. M. Urbassek, Nucl. Instrum. Methods Phys. Res. B **30**, 507 (1988).
[27] H. M. Urbassek and U. Conrad, Nucl. Instrum. Methods Phys. Res. B **69**, 413 (1992).
[28] H. M. Urbassek and J. Michl, Nucl. Instrum. Methods Phys. Res. B **22**, 480 (1987).
[29] P. Sigmund, in *Sputtering by particle bombardment I*, edited by R. Behrisch (Springer, Berlin, 1981), p. 9.
[30] H. H. Andersen, Mat. Fys. Medd. K. Dan. Vidensk. Selsk. **43**, 127 (1993).
[31] E. Salonen, K. Nordlund, and J. Keinonen, Nucl. Instrum. Methods Phys. Res. B **212**, 286 (2003).